

## Beam Scattering Through Foil at NSRL

B. Dhital

March 2024

Collider Accelerator Department  
**Brookhaven National Laboratory**

**U.S. Department of Energy**

USDOE Office of Science (SC), Nuclear Physics (NP)

Notice: This technical note has been authored by employees of Brookhaven Science Associates, LLC under Contract No. DE-SC0012704 with the U.S. Department of Energy. The publisher by accepting the technical note for publication acknowledges that the United States Government retains a non-exclusive, paid-up, irrevocable, world-wide license to publish or reproduce the published form of this technical note, or allow others to do so, for United States Government purposes.

## **DISCLAIMER**

This report was prepared as an account of work sponsored by an agency of the United States Government. Neither the United States Government nor any agency thereof, nor any of their employees, nor any of their contractors, subcontractors, or their employees, makes any warranty, express or implied, or assumes any legal liability or responsibility for the accuracy, completeness, or any third party's use or the results of such use of any information, apparatus, product, or process disclosed, or represents that its use would not infringe privately owned rights. Reference herein to any specific commercial product, process, or service by trade name, trademark, manufacturer, or otherwise, does not necessarily constitute or imply its endorsement, recommendation, or favoring by the United States Government or any agency thereof or its contractors or subcontractors. The views and opinions of authors expressed herein do not necessarily state or reflect those of the United States Government or any agency thereof.

# Beam Scattering Through Foil at NSRL

Bhawin Dhital,\* Kevin Brown, Michael Sivertz, Nicholas Tsoupas, Trevor Olsen, David Inzalaco, and Petra Adams  
*Brookhaven National Laboratory, Upton NY 11973*

David Sagan and Weijian (Lucy) Lin  
*Cornell University*  
(Dated: April 9, 2024)

In this note, we describe the foil structure that is used in the NASA Space Radiation Laboratory (NSRL) transport line just before D6 septum magnet. Foils of different materials and thickness are used through which different ion species at different energies pass. Foil removes the electrons from the incoming ions and make it fully stripped (*or partially stripped is also possible*). Further, when charged particles pass through a foil, the outgoing particles form a Gaussian like angular distribution. This Gaussian like distribution passes through a set of octupole magnets creates a uniform beam distribution at the NSRL target which is required for various beam experiments. We utilize the Bmad and SRIM packages to calculate the energy loss through the foils for various ion species at different energies and charge states. Finally, we provide a summary of the energy loss calculations through the foils using these two different methods.

## I. INTRODUCTION

The idea of using the foil along the NASA Space Radiation Laboratory (NSRL) beam line has mainly two advantages: first, it reduces the rigidity of the transported beams, and second, the multiple scattering of the ion beams at the foil generates the Gaussian angular distribution which is required for generating a uniform beam distribution at the NSRL target [1, 2].

When charged particles pass through a thin medium foil, the outgoing particles form a Gaussian like angular distribution [3]. In our studies, charged particles are protons and ions at different energies. Scattering process is dominated by screened Coulomb interaction between the projectiles (protons and ions) and target atom (Copper and Aluminium foils). We will discuss the scattering process along with the energy loss mechanism of ions passing through the foil material in the transport line.

In this note, we calculate the multiple scattering of protons and ions incident upon copper and aluminium foils and compare the results calculated from Bmad [4] and SRIM [5, 6]. In Bmad, a foil element represents a planar sheet of material which strips electrons from an incoming particle towards it. In conjunction, there will be scattering of the particle trajectory as well as an associated energy loss [4].

## II. ACCELERATOR OVERVIEW

### A. Booster Synchrotron

The booster synchrotron was designed to accelerate protons and heavy ions [2]. It is a 201.78 m circumference separated function alternating gradient synchrotron

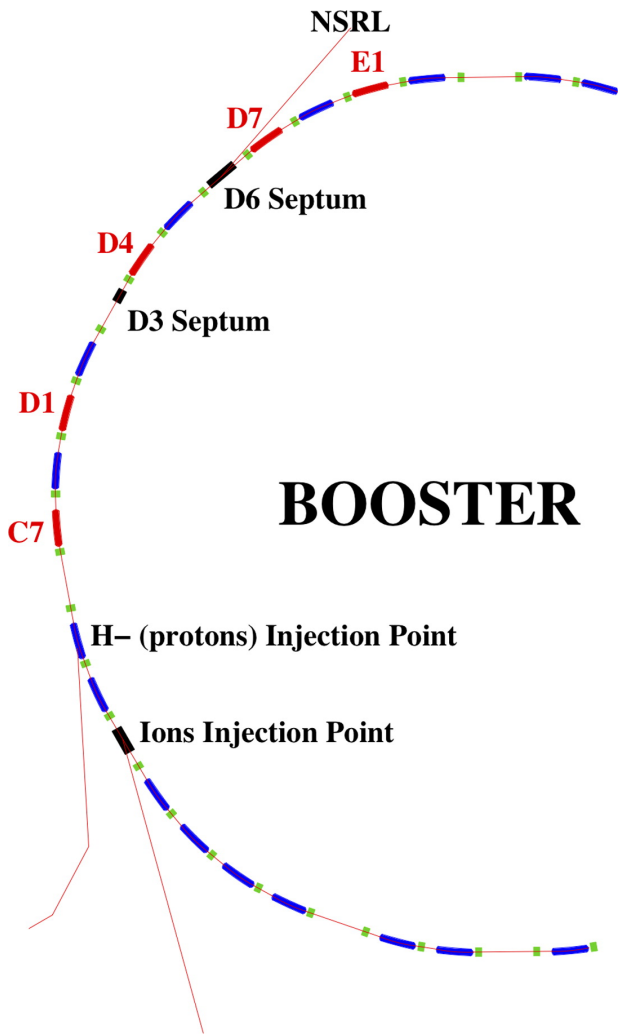
that can operate up to a maximum rigidity of 17 Tm. Booster ring is composed of 36 sector magnet dipoles and 48 quadrupoles. All magnets are iron-dominated and water cooled. The main dipoles are 2.34 m in (physical) length. Quadrupoles are of two types with (physical) lengths of 0.4255 and 0.4382 m. The vacuum chamber in the dipoles has dimensions  $70 \times 150 \text{ mm}^2$  and in the quadrupoles is 152 mm (circular). The nominal betatron tunes are 4.82, horizontal, and 4.83, vertical. The booster is logically divided into six super-periods, labeled A through F. Each super-period contains six dipoles and eight quadrupoles, with two long straight sections (the third and sixth locations of every superperiod). These straight sections are used to contain radio frequency (RF) accelerating cavities, injection devices, and extraction devices [2]. For one-third resonance extraction from the booster ring to the NSRL line, we have five bump magnets, two septa magnets and two families of sextupoles placed at different regions of the booster ring. D3 is a thin septum magnet with effective thickness of 0.76 mm and maximum kick of 3 mrad, for a length of 1 m. The thick septum D6 has an effective thickness of 15.2 mm, is operated in a dc mode, and gives a kick of 155 mrad, for a length of 2.5 m [7]. Those extraction sextupole magnets are different than those sextupole magnets being used to correct the chromaticity in the ring. The layout of the booster ring with five bumps and two septa magnets is shown in Fig. 1a.

### B. The NSRL Facility

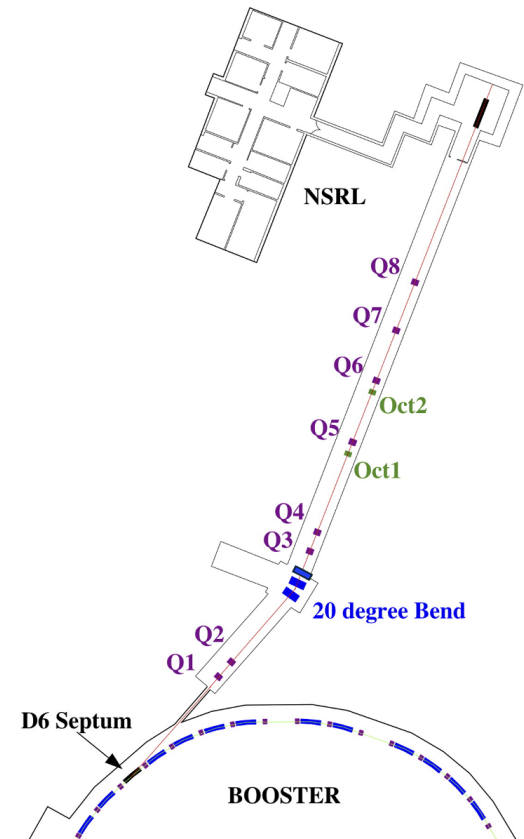
The various ions are delivered to the NSRL facility from a single beam transport line that branches off from the booster. Ions for NSRL are extracted from the booster using one of two methods; resonant slow extraction or fast extraction. In this note, our main focus is on the slow extraction method. The slow extraction system consists of two septa magnets, five bump magnets, and

---

\* bdhital@bnl.gov



(a) Layout of the portion of the booster ring showing five extraction bumps and two extraction septa magnets D3 and D6.



(b) Layout of the NSRL beam line starting at D6 septum [2].

four sextupole magnets [7–9].

The schematic layout of the NSRL beam line is shown in Fig. 1b. The NSRL line consists of three dipoles forming a  $20^\circ$  bend (rarc-20), nine quadrupoles (Q1–Q9) magnets (Q9 is not shown in Fig. 1b), and two octupole (Oct1 & Oct2) magnets respectively. The two octupoles, one upstream of Q5 and the other upstream of Q6, can be adjusted to achieve a uniform rectangular distribution of beam on target. The optics of the line is designed to make an achromatic beam after a  $20^\circ$  bend dipoles. This is crucial towards achieving good quality uniform beams since momentum dependent motion at the entrance to the octupoles will affect the uniformity.

### III. RESONANCE EXTRACTION

The slow extraction system consists of two septa magnets, five bump magnets, and four sextupole magnets.

This has been described and reported on in Refs. [7, 8, 10]. Resonant extraction begins by inducing a resonant condition within the accelerator, achieved through the activation of two sets of sextupole magnets. These magnet sets operate with opposing polarities, effectively nullifying their chromatic effects on the lattice to a first-order approximation. Once this resonance condition is established, particle betatron frequencies approach approximately  $13/3$  oscillations per revolution, initiating a nonlinear increase in particle amplitudes. Over several hundred to several thousand revolutions, transverse deviations of particle trajectories from the nominal orbit escalate to the point where the amplitude from one turn to the next exceeds the thin septum's thickness significantly (approximately five times larger). Consequently, the majority of particles traverse the septum and enter the magnetic deflection field. Any particles inadvertently colliding with the septum are lost.

The septum magnets, acting as dipoles, are situated

within the Booster D3 and D6 straight sections. The D3 magnet features a thin septum, approximately 0.76 mm thick, which serves as the initial barrier encountered by the resonant beam. Upon crossing this septum, ions are deflected by its magnetic field towards the magnetic aperture of the D6 septum magnet. This magnet, with an effectively thicker septum measuring about 15.2 mm, further guides the particles into the NSRL beam line. Prior to reaching the D6 magnet, ions that have traversed the D3 septum pass through a foil where any remaining electrons are stripped away. This stripping process reduces ion rigidity, thereby diminishing the magnetic field required in both the D6 magnet and the NSRL transport line [2].

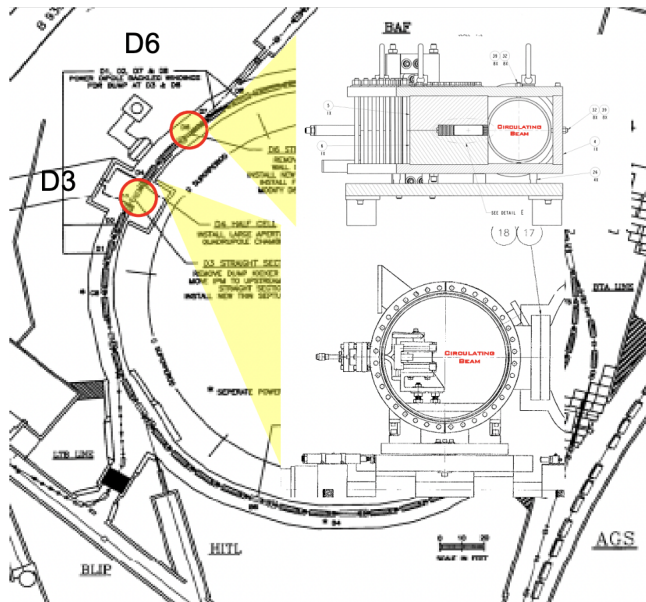


FIG. 2: Layout of the booster ring with D3 and D6 septa magnets.

#### IV. FOIL ELEMENT

A foil element represents a planar sheet of material which can strip electrons from a particle. In conjunction, there will be scattering of the particle trajectory as well as an associated energy loss [4]. The different types of foils are being used in the beam line and analysis from beam studies with stripping foils have been performed [11]. Each ion beam is usually stripped of its electrons by a foil which is located at the entrance of the NSRL beam line, just before D6 septum and can be inserted and retracted automatically from the path of the beam [1]. The NSRL beam line has foil thickness is typically 0.1mm. In the later section, we will discuss scattering through the foil. Finally, we calculate the energy loss through foils for different ion species at different energies. A comparison on energy loss calculated using



FIG. 3: Physical D6 septum magnet with foil stripper at the beginning of the NSRL transport line.

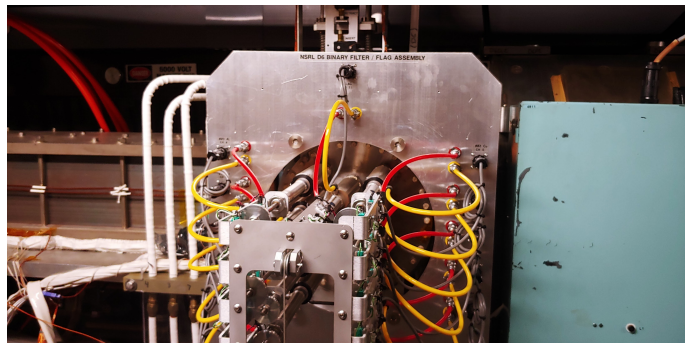


FIG. 4: D6 foil unit.

Bmad and SRIM will be presented.

#### A. Scattering through Foil

A charged particle traversing a medium is deflected by many small-angle scatters [12]. Most of the deflections of incoming ions particles are due to Coulomb scattering from nuclei of target (foil) as described by the Rutherford cross section. Hence from the central limit theorem, for many small-angle scatters the net scattering and displacement distributions are Gaussian. Also Coulomb scattering process are well described by some theories [13, 14].

We define the scattering angle ( $\sigma$ ) following Gerald R. Lynch and Orin Dahl [15]. The expression for the scattering angle becomes

$$\sigma = \frac{S_z z}{p\beta} \sqrt{\frac{X}{X_0}} \left[ 1 + \varepsilon \log_{10} \left( \frac{Xz^2}{X_0\beta^2} \right) \right]. \quad (1)$$

Here  $p$ ,  $\beta$ , and  $z$  are the momentum, speed, and the charge number of the incident particle, and  $X/X_0$  is the

thickness of the scattering medium in radiation length. This form takes into account the  $\beta$  and  $z$  dependence quite well at small  $z$ , but for large  $z$  and small  $X$  the  $\beta$ -dependence is not taken into account very well. The other parameters  $S_z$  and  $\varepsilon$  and their values are explained in details in the reference [15].

High-energy electrons mostly lose energy in matter by bremsstrahlung, and high-energy photons by  $e^+e^-$  pair production. The characteristic amount of matter traversed for these related interaction is called the radiation length  $X_0$ , usually measured in  $\text{g}/\text{cm}^2$ . In other words, it is the mean distance over which a high-energy electron loses all but  $1/e$  of its energy by bremsstrahlung. In our calculation, we express the radiation length in the unit of  $\text{kg}/\text{m}^2$ . The value of  $X_0$  for different materials has been calculated and tabulated by Y.S. Tsai [16]. Mathematically, the expression for the radiation length  $X_0$  is given by

$$\frac{1}{X_0} = 4\alpha r_e^2 \frac{N_A}{A} \{Z^2[L_{rad} - f(Z)] + ZL'_{rad}\}. \quad (2)$$

For  $A = 1 \text{ g mol}^{-1}$ ,  $4\alpha r_e^2 N_A/A = (716.408 \text{ g cm}^{-2})^{-1}$ .  $L_{rad}$  and  $L'_{rad}$  are given in Table I. The function  $f(Z)$  is an infinite sum, but for elements up to uranium can be represented to 4-place accuracy by

$$f(Z) = a^2[(1+a^2)^{-1} + 0.20206 - 0.369 a^2 + 0.0083 a^4 - 0.002 a^6] \quad (3)$$

where  $a = \alpha Z$  [17].  $\alpha$  is the fine structure constant.

TABLE I:  $L_{rad}$  and  $L'_{rad}$  used in calculating the radiation length.

Element	Z	$L_{rad}$	$L'_{rad}$
H	1	5.31	6.144
He	2	4.79	5.621
Li	3	4.74	5.805
Be	4	4.71	5.924
Others	>4	$\ln(184.15 Z^{-1/3})$	$\ln(1194 Z^{-2/3})$

In Eq. (1), the foil thickness  $X$  should be either in cm or m. To make the quantity  $X/X_0$  dimensionless,  $X$  should be multiplied by the material density so it takes the unit of  $\text{gm}/\text{cm}^2$  or  $\text{kg}/\text{m}^2$ . We take SI unit convention of  $\text{kg}/\text{m}^2$  for  $X$  in our calculations.

Further, the particles angular distribution change after passing through the foil. If  $(x_p, y_p)$  are the transverse coordinates of a incoming particle before the foil, then after foil the new co-ordinates  $(x'_p, y'_p)$  become

$$\begin{aligned} x'_p &= x_p + r_1(x) * \sigma \\ y'_p &= y_p + r_2(y) * \sigma. \end{aligned} \quad (4)$$

Here,  $r_1, r_2$  function return a normally distributed distribution since we know that foil generates the normal distribution of particles passing through it.

Hence, the Gaussian beam distribution at D6 septum (beginning of the NSRL line) as shown in Fig. 5c can be focused magnetically along the beam transport line using a set of different magnets to create a uniform beam at the target.

## B. Energy Loss through Foil

Low energies electrons and positrons primarily lose energy by ionization. Although there are some other scattering process that may contribute to the energy loss. Bethe formula is highly used to describe the mean energy loss per distance travelled by charged particles traversing matter. The charged particles moving through matter interact with the electrons if atoms in the target material (foil). This interaction excites or ionize the atoms, which leads to the energy loss of the traveling particles.

For a particle with speed  $v$ , charge  $z$ , and energy  $E$ , traveling a distance  $x$  into a foil target if electron number density  $n$  and mean excitation energy  $I$ , the relativistic formula to calculate the energy loss is given by[18]

$$-\left\langle \frac{dE}{dx} \right\rangle = \frac{4\pi}{m_e c^2} \cdot \frac{nz^2}{\beta^2} \cdot \left( \frac{e^2}{4\pi\epsilon_0} \right)^2 \cdot \left[ \log_{10} \left( \frac{2m_e c^2 \beta^2}{I(1-\beta^2)} \right) - \beta^2 \right], \quad (5)$$

where  $c$  is the speed of light,  $\epsilon_0$  is the vacuum permittivity,  $\beta = v/c$ ,  $e$ , and  $m_e$  are electronic charge and rest mass of electron respectively. The electron density  $n$  of the material can be calculated by using the following formula

$$n = \frac{N_A \cdot Z \cdot \rho}{A \cdot M_u}, \quad (6)$$

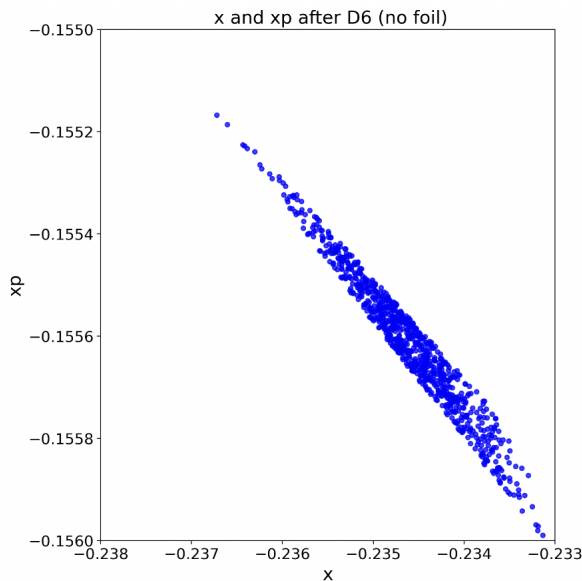
where  $N_A$  is the Avogadro number,  $Z$  its atomic number,  $\rho$  is the density of the material,  $A$  is its relative atomic mass, and  $M_u$  is the molar mass constant. The total energy loss through foil  $\Delta E$  is then calculated multiplying  $-\left\langle \frac{dE}{dx} \right\rangle$  by  $dx$ , the total foil thickness.

## V. ENERGY LOSS CALCULATIONS

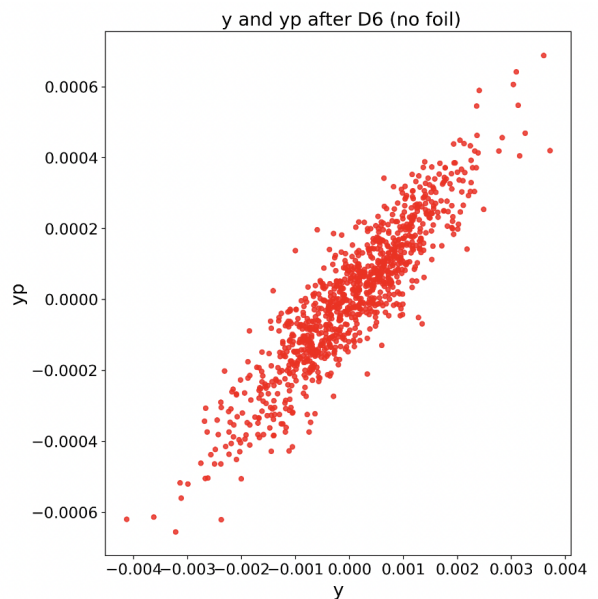
We calculate the energy loss through foil elements of different thickness using Bmad and SRIM. The Table III shows the states of some of the ions before and after they are stripped of electrons respectively.

### A. Bmad Model

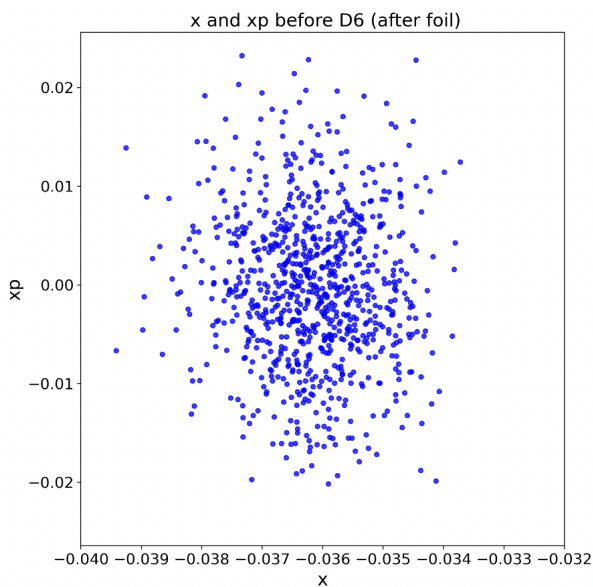
As mentioned in subsection IV B, Bmad uses Bethe formula given by Eq. (5) to calculate the energy loss through foils of different materials. We have used copper and aluminium foils with different thickness and protons and ions beams at different energies passing through them.



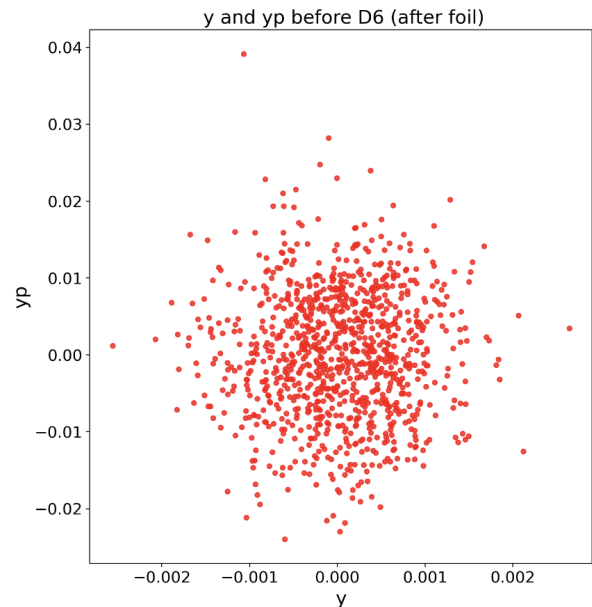
(a) Horizontal phase space ( $x, xp$ ) before D6 septum in the absence of foil.



(b) Vertical phase space ( $y, yp$ ) before D6 septum in the absence of foil.



(c) Horizontal phase space ( $x, xp$ ) before D6 septum after passing through foil at the beginning of NSRL transfer line.



(d) Vertical phase space ( $y, yp$ ) before D6 septum after passing through foil at the beginning of NSRL transfer line.

FIG. 5: Transverse beam phase-space distribution before and after the foil. Proton beam energy of 1000 MeV with 1000 particles being used in the tracking simulation through Copper (Cu) foil of thickness 0.2032 mm.

The ion species, their kinetic energy, individual foil thickness, and energy loss values are presented in Table II. The Bmad foil set-up example is given in Appendix A.

## B. SRIM model

Further, we calculate the energy loss through foil using NSRL StackUp Calculator, also called **SRIM** and it stands for **S**topping and **R**ange of **I**ons in **M**atter. The excel-based SRIM calculator can be downloaded from the website : <https://www.bnl.gov/nsrl/stackup/>.

TABLE II: Energy loss through foils for various ion species at different energies. All energies are in MeV/n.

Ion	K.E.(Booster)	Cu foil (mm)	Al foil (mm)	Total foil thickness (mm)	$\Delta E$ (Bmad)	$\Delta E$ (SRIM)
H	1002	0.2032	0.0	0.2032	0.25	0.26
C	303.5	0.1016	0.0127	0.1143	0.67	0.66
Fe	1017	0.6858	0.00635	0.69215	11.82	10.95
Nb	441.5	0.2286	0.0127	0.23495	7.35	7.24
Tb	402	0.254	0.0	0.254	12.55	11.92
Au	269	0.1524	0.0127	0.1651	11.32	11.05
Bi	147	0.2032	0.00635	0.20955	22.91	21.51

TABLE III: Ion Species with initial and final charge states used in NSRL.

Ion Species	$Q_{foil,in}$	$Q_{foil,out}$	Total Nucleons (N)
H	+1	+1	2
He	+2	+2	4
C	+5	+6	12
O	+7	+8	16
Si	+11	+14	28
Ti	+17	+22	48
Fe	+20	+26	56
Nb	+23	+41	93
Ag	+29	+47	108
Tb	+35	+65	159
Ta	+38	+73	181
Au	+32	+79	197
Bi	+43	+83	209

A database of energy, range,  $dE/dx$ , and straggling information has been assembled for all ions available at NSRL and more across a selection of materials traditionally used by the heavy ion radiation field. This database is an extraction from the Stopping and Range of Ions in Matter (SRIM/TRIM) free software by J. F. Ziegler. More information about the SRIM software can be found at [www.SRIM.org](http://www.SRIM.org). A GUI window of SRIM to calculate energy loss through foil is given in Appendix B.

## VI. DISCUSSION

We calculated the energy loss through foils of different materials using Bmad and SRIM for various ion species at different energies. The calculations show that the energy loss values calculated by Bmad and SRIM are in good agreement for ions at different energy levels. However, we observed that the energy loss values calculated by Bmad tend to overshoot those calculated by SRIM, especially for heavier ions. Bmad utilizes the Bethe formula to calculate the energy loss through foils of different materials, making it a more theoretical model. Conversely,

energy loss calculations in SRIM are based on sophisticated models and algorithms grounded in established theories of ion-solid interactions, which have been extensively validated against experimental data, providing confidence in their accuracy and reliability.

Additionally, we conduct particle tracking simulations using Bmad, employing 1000 particles for the simulation. Before passing through the foil, the transverse phase space distribution is non-Gaussian, attributed to the slowly extracted beam from the booster synchrotron. However, after traversing the foil, the transverse phase space distribution transforms into a Gaussian distribution. This Gaussian beam distribution, upon passing through various magnets along the NSRL beamline, facilitates the creation of uniform beam distributions at the NSRL target. This uniform distribution is crucial for meeting the requirements of various beam experiments.

## ACKNOWLEDGMENTS

The work is supported by Brookhaven Science Associates, LLC, under Contract No. DE-SC0012704 with the U.S. Department of Energy and by NASA (Contract No. T570X).



## Appendix A: Foil Set-Up in Bmad

```

parameter[geometry] = Open
! Bismuth ion
!#### Bi43 147 MeV, 8.25 mils, Cu = 0.0002032 m,
!Al = 6.35e-6 m
beginning[e_tot] = 209*1085000000.0 !eV, 147 MeV
parameter[particle] = #209Bi+43
final_charge =+83

parameter[n_part] =1

!=====
! Initial twiss conditions
!=====

beginning[beta_a] = 9.17
beginning[beta_b] = 6.315
beginning[alpha_a] = -1.48
beginning[alpha_b] = 1.085
beginning[eta_x] = 0
beginning[eta_y] = 0

```

```

!=====
! particle co-ordinates
!=====
particle_start[x] = 0.001
particle_start[px] = 0.002
particle_start[y] = 0.003
particle_start[py] = 0.004
particle_start[z] = 0.005
particle_start[pz] = 0.00

!#### Bi43 147 MeV, 8.25 mils, Cu = 0.0002032 m,
!Al = 6.35e-6 m
fl1:foil,material_type="Cu", thickness=0.0002032
fl2:foil,material_type="Al", thickness=6.35e-6
ln:line=(fl1,fl2)
use,ln

```

## Appendix B: SRIM GUI To Calculate Energy Loss Through Foil

- 
- [1] N. Tsoupas, L. Ahrens, S. Bellavia, R. Bonati, K. Brown, I.-H. Chiang, C. Gardner, D. Gassner, S. Jao, W. Mackay, *et al.*, Physical Review Special Topics-Accelerators and Beams **10**, 024701 (2007).
- [2] K. Brown, L. Ahrens, I. H. Chiang, C. Gardner, D. Gassner, L. Hammons, M. Harvey, N. Kling, J. Morris, P. Pile, *et al.*, Nuclear Instruments and Methods in Physics Research Section A: Accelerators, Spectrometers, Detectors and Associated Equipment **618**, 97 (2010).
- [3] T. Yamazaki, M. Takasaki, and M. Sakisaka, Journal of the Physical Society of Japan **36**, 1643 (1974).
- [4] D. Sagan, Nuclear Instruments and Methods in Physics Research Section A: Accelerators, Spectrometers, Detectors and Associated Equipment **558**, 356 (2006).
- [5] J. F. Ziegler and J. P. Biersack, in *Treatise on Heavy-Ion Science: Volume 6: Astrophysics, Chemistry, and Condensed Matter* (Springer, 1985) pp. 93–129.
- [6] J. F. Ziegler, M. D. Ziegler, and J. P. Biersack, Nuclear Instruments and Methods in Physics Research Section B: Beam Interactions with Materials and Atoms **268**, 1818 (2010).
- [7] K. Brown, J. Cullen, J. Glenn, Y. Lee, A. McNerney, J. Niederer, T. Roser, A. Soukas, J. Tuozzolo, and N. Tsoupas, in *Proceedings of the 1999 Particle Accelerator Conference (Cat. No. 99CH36366)*, Vol. 2 (IEEE, 1999) pp. 1270–1272.
- [8] K. Brown, J. Cullen, J. Glenn, M. Mapes, I. Marneris, N. Tsoupas, L. Snyderstrup, and W. van Asselt, in *PACS2001. Proceedings of the 2001 Particle Accelerator Conference (Cat. No. 01CH37268)*, Vol. 2 (IEEE, 2001) pp. 1517–1519.
- [9] N. Tsoupas, S. Bellavia, R. Bonati, K. Brown, I. Chaing, C. Gardner, S. Jao, I. Marneris, A. Marneris, D. Phillips, *et al.*, in *Proceedings of the 2004 European Particle Accelerator Conference, Luzern* (2004).
- [10] K. Brown, L. Ahrens, S. Bellavia, S. Binello, B. Brelford, D. DuMont, W. Eng, C. Gardner, D. Gassner, J. Glenn, *et al.*, in *Proceedings of the 2003 Particle Accelerator Conference*, Vol. 3 (IEEE, 2003) pp. 1542–1544.
- [11] G. Marr, L. Ahrens, P. Thieberger, and K. Zeno, *Analysis from Beam Studies with BTA Stripping Foils*, Tech. Rep. (Brookhaven National Lab.(BNL), Upton, NY (United States). Relativistic Heavy . . . , 2003).
- [12] D. E. Groom and S. Klein, The European Physical Journal C-Particles and Fields **15**, 163 (2000).
- [13] H. A. Bethe, Physical review **89**, 1256 (1953).
- [14] C. Case and E. Battle, Physical Review **169**, 201 (1968).
- [15] G. R. Lynch and O. I. Dahl, Nuclear Instruments and Methods in Physics Research Section B: Beam Interactions with Materials and Atoms **58**, 6 (1991).
- [16] Y.-S. Tsai, Rev. Mod. Phys. **46**, 815 (1974).
- [17] H. Davies, H. A. Bethe, and L. C. Maximon, Phys. Rev. **93**, 788 (1954).
- [18] J. D. Cockcroft, Nature **175**, 53 (1955).

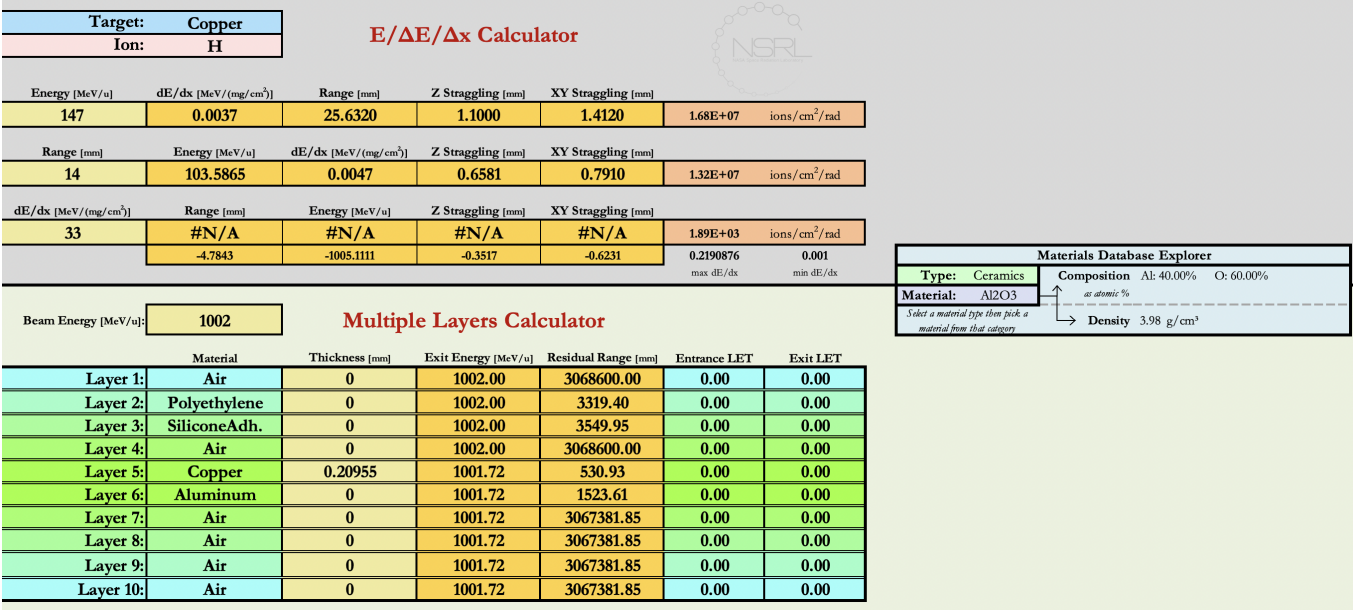


FIG. 6: SRIM GUI for 1002 MeV proton beams scattering through copper foil of thickness 0.2095 mm.